A Numerical Revisit on Mass Transfer Experiments at a Free Surface in a Turbulent Open Channel Flow

Ryuichi Nagaosa
Institute of Environmental Management Technology (EMTech), AIST Tsukuba West, 16-1 Onogawa, Tsukuba, 305-8569, Japan

This study deals with mechanism of gas transport into a turbulent liquid across a shear-free gas-liquid interface (or free surface) in an open channel. A direct numerical simulation of three-dimensional Navier-Stokes and gas transport equations is applied to realize three-dimensional turbulent flows in a region close to the free surface. The Reynolds number defined by the wall shear velocity and the water height is varied from 150 to 400 to consider the effect of the Reynolds number on turbulent gas transport. The gas transfer coefficient at the free surface is evaluated by the ensemble-average of instantaneous three-dimensional gas concentration distribution. The results of the present numerical simulations are compared with the previous laboratory experiments on the gas transfer coefficient. The comparison of between the laboratory experiments shows that the absolute values of the Sherwood number, which is a normalized form of the gas transfer coefficient, predicted by the present DNS agree well those obtained by the previous laboratory experiments. While the present numerical predictions reveal that Sh is proportional to 3/4 power of the Reynolds number defined by the bulk mean velocity, Re_m, the previous laboratory experiments concluded that $Sh \propto Re_m$ is satisfied, resulting overestimation of Sh at large Reynolds number region in the laboratory experiments. Several reasons for the discrepancy between the laboratory and numerical experiments could be point out. In particular, the effect of small-scale perturbation on the free surface produced by the experimental equipment for measuring gas flux is thought critical for the overestimation of gas flux. In addition, this report proposes a new definition for the characteristic time scale, instead of applying the previous VITA method for evaluation of the time scales of the surface renewal. The length scales of the surface divergence are computed by their two-point correlation in the streamwise direction, and the characteristic time scales are obtained by using the length scales. The results of the time scale analysis reveal that the time scales of the surface divergence obeys the surface renewal assumption, asserting that the surface divergence is one of the candidates to quantify the gas fluxes at the free surface.

INTRODUCTION

A research on gas transfer mechanism at a gas-liquid interface has been under active investigation particularly in the last two decades. This research has been motivated by the necessity for evaluating gas fluxes at the atmosphere-ocean interface in related to understanding, for example, global carbon cycle, and manipulation of gas fluxes in industrial equipment. An investigation on turbulence and turbulent gas transfer at a shear-free gas-liquid interface (or free surface) in a two-dimensional channel is expected to dedicate for fundamental understanding on physics of turbulent gas transport, since turbulence in the open channel is one of the most simplified flows with the free surface. The author has investigated relation between turbulence structures and turbulent gas transfer mechanism at the free surface in the open channel experimentally and numerically in the last decade. We found throughout the laboratory experiments on measurements of turbulence structures and turbulent gas transport that the gas transfer mechanism is determined by interactions of turbulence with the free surface. The idea of the surface renewal introduced by Dankwerts[1]

was employed to quantify the free surface activity for gas transport, and an empirical correlation for gas transfer at the free surface are made based on this idea by measuring the surface renewal frequency in the laboratory experiments. The empirical correlation suggests that the gas flux at the free surface is proportional to square of the surface renewal frequency, which is consistent with the concept by Dankwerts. Also, Rashidi et al.[2] measured the free-surface activity, defined by the fraction of the free-surface area covered by turbulent patch, and the mean patch residence time at the free surface. They correlated the gas flux with these hydrodynamic properties based on the surface renewal approximation, and compared the predicted gas fluxes with those measured by Komori et al.[3,4] The comparison exhibited that the Rashidi et al. prediction agrees well with our previous measurements of gas fluxes. Rashidi[6] observed turbulence-surface interactions by their flow visualization approach based on a hydrogen-bubble technique, and found that the near-wall turbulence is an origin of the turbulent patch on the free surface. Recently, Nagaosa and Handler[6] confirmed numerically that the near-wall coherent structures emanate toward the free surface and induce the splat events.

Although the idea of the surface renewal assumption seems to be helpful for evaluation of the gas transport mechanism, quantification of the surface renewal events needs conditional sampling technique. It suggests that condition for sampling data should be specified, hence, optimization of parameters for data sampling is inevitable. For instance, Komori et al.[3,4] applied the variable-time time averaging (VITA) technique[7] to educe the surface renewal from dye tracer signals. In their detection process, two parameters should be optimized; one is the averaging time for taking the local average of the signals, and the other is the threshold level to discern the surface renewal motions from background random perturbation. An appropriate determination of the two parameters will be difficult to generalize, and will not be practical in various kinds of turbulent flows. Also, quantification of the area covered by turbulent patch and its mean residence time as Rashidi et al.[2] carried out in their study are also difficult, depending on their definition. These definitions were not discussed in the Rashidi et al. report[2], and ambiguity for quantification of both the patch area fraction and the mean patch residence time remains.

This study concentrates on quantifying the free-surface activity by introducing the surface divergence. This parameter is expected to quantify exactly the free-surface activity, which is synchronized by presence of splat (a fluid motion moving toward the free surface) and anti-splat (a fluid motion moving away from the free surface) events[8]. One of the benefits for introducing this hydrodynamic parameter is easy evaluation of this parameter in numerically simulated turbulence. This parameter involves spatial derivatives in a two-dimensional free surface, and its evaluation was almost impossible based on traditional equipment for turbulence measurements such as a laser-Doppler velocimetry and a hot-wire probe. A digital particle image velocimetry, however, has been employed for multidimensional turbulence measurements, and this tool is expected to overcome the previous difficulties in measuring the surface divergence.

The purpose of this study is to discuss turbulence structures and turbulent gas transport mechanism at the free surface in fully developed turbulence. We employ a direct numerical simulation technique to examine physics of free-surface turbulent flows. For validation of the present numerical approach, the results of the laboratory measurements on gas flux were used for comparison. Several turbulence statistics on the surface divergence are shown to discuss characteristic length and time scales. Suitability of the surface divergence to predict gas fluxes at the free surface is explained by showing the joint probability density distributions of the surface divergence and the concentration gradient at the free surface.

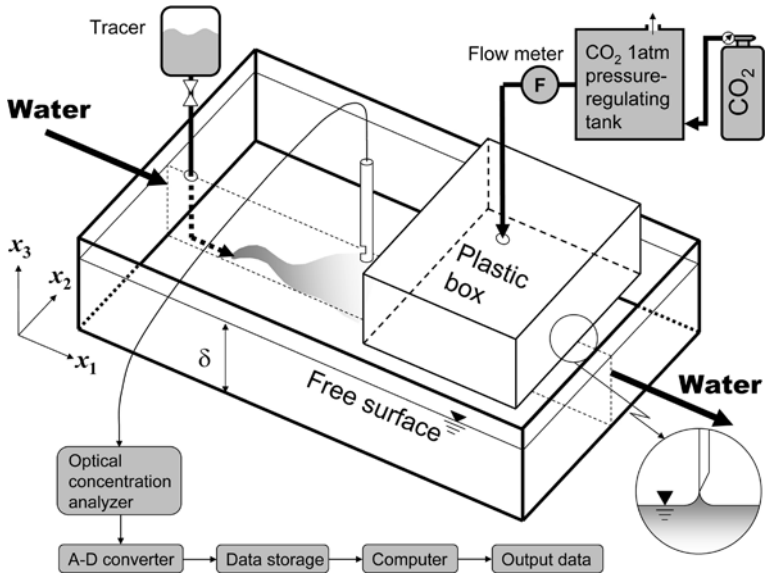

Figure 1: Experimental apparatus for measuring gas flux and subsurface hydrodynamics in turbulent open channel flows.

LABORATORY EXPERIMENTS

Figure 1 illustrates experimental setup for measurement of gas fluxes at the free surface in the open channel.[3,4] The dimensions of the open channel are 7.6 m long, 0.5 m width and 0.2 m height. The laboratory experiments have been carried out in a range of the Reynolds number of about $2{,}600 < \mathrm{Re}_m < 12{,}200$, where Re_m is the Reynolds number defined by the bulk mean velocity, $U_m \equiv \delta^{-1}\int_0^\delta \langle u_1 \rangle dx_3$, the water depth, δ and fluid viscosity, ν, as $\mathrm{Re}_m = U_m\delta/\nu$ ($\langle . \rangle$ signifies the time-space average). The Reynolds number Re_m can be converted to the friction Reynolds number, Re, based on the wall shear velocity, u_τ, by applying the empirical correlation of the viscous friction coefficient at the wall by Dean[9]

$$f = 0.073\left(2\mathrm{Re}_m\right)^{-1/4}. \tag{1}$$

Substituting Eq. (1) into the definition of the viscous friction coefficient,

$$\tau_w = \rho u_\tau^{\,2} = \frac{f}{2}\rho U_m^{\,2}, \tag{2}$$

we obtain the relation between $\mathrm{Re} \equiv u_\tau\delta/\nu$ and Re_m as

$$\mathrm{Re} = 0.175\mathrm{Re}_m^{\,7/8}, \tag{3}$$

where ρ is the fluid density. Using Eq. (3), the experimental Reynolds number regime of $2{,}600 < \mathrm{Re}_m < 12{,}200$ corresponds to about $170 < \mathrm{Re} < 660$. The Froude numbers in the laboratory measurements are changed from approximately 0.1 to 0.7, where the Froude number is defined by $\mathrm{Fr} \equiv U_m/(g\delta)^{1/2}$ based on the gravitational acceleration, g. The hydrolically subcritical condition of the laboratory experiments suggests that the effect of wave activity at the free surface does not play an important role in determining turbulence structures in water.

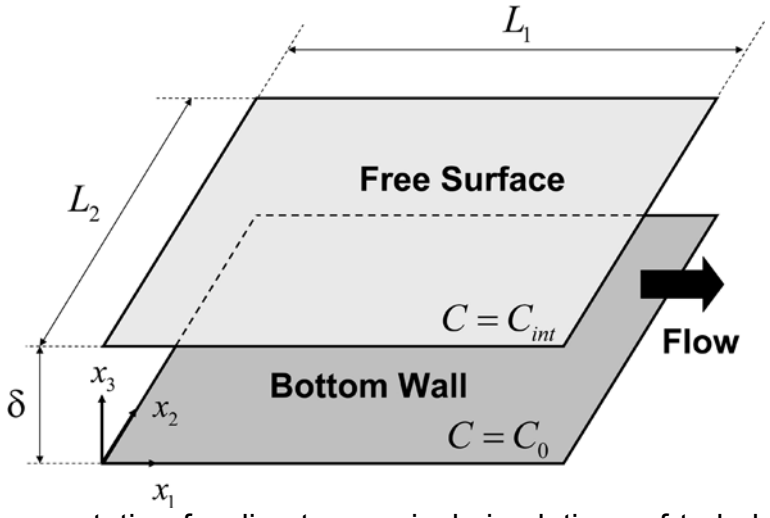

Figure 2: Schematic representation for direct numerical simulations of turbulent open channel flows.

We use carbon dioxide (CO_2) to measure gas fluxes at the free surface, since this gas has relatively large solubility into water at standard temperature and pressure and gas-liquid equilibrium in water-CO_2 system obeys the Henry's law,

$$p_{CO_2} = HC_{\text{int}}, \tag{4}$$

where p_{CO_2} is the partial pressure of CO_2 in the atmosphere above the free surface, and H is the Henry constant. The molecular diffusivity of CO_2 in water is $1.74\times10^{-9}\ \text{m}^2/\text{s}$ at $293\,\text{K}$, therefore, the Schmidt number in the laboratory experiments is $\text{Sc} \approx 580$ at this temperature. A plastic box of 1.0 m long and 0.3 m width filled with CO_2 is installed above the free surface, so that flow rate of CO_2 absorbed into turbulent water is measurable based on a soap-film meter equipped as indicated in Figure 1. Since this plastic box is sealed by very thin water film due to the effect of capillary at the water surface, pressure in this plastic box is always maintained constant at an atmospheric pressure of about $p_{CO_2} \approx 101.3\,\text{kPa}$. Once we determined gas flux at the free surface, the gas transfer coefficient, K, is determined by

$$Q = K\left(C_{\text{int}} - C_0\right), \tag{5}$$

where gas concentration at the wall is assumed to be zero, $C_0 = 0$.

NUMERICAL METHOD

Figure 2 is the schematic representation of the computational domain for turbulent open channel flows. We consider a rectangular box bounded by a solid bottom wall and a rigid free surface to realize fully developed turbulence.[10] The sizes of the computational domain are L_1, L_2 and δ in the streamwise, spanwise and wall-normal directions. The periodic boundary condition is applied to both the streamwise and spanwise directions to generate fully developed turbulence. The bottom is treated as a non-slip boundary, while a free-slip assumption is used for approximating the free surface under zero-Froude number assumption. Suitability of the zero-Froude number assumption has been certified by our previous numerical studies on turbulence in the open channel[10].

Table 1: Outline of direct numerical simulations.

Run	Re	U_m	Re_m	Sh	$L_1 \times L_2$	Grid Points	Δx_1^+	Δx_2^+	Δx_3^+
I	150	15.3	2,290	4.70	$4\pi\delta \times 2\pi\delta$	192×256×97	9.82	3.68	0.183~3.49
II	180	15.7	2,830	5.50	$4\pi\delta \times 2\pi\delta$	256×288×109	8.84	3.93	0.174~3.83
III	240	16.4	3,930	7.09	$2.5\pi\delta \times 1.25\pi\delta$	192×256×137	9.82	3.68	0.168~4.14
IV	300	17.0	5,100	8.50	$2\pi\delta \times \pi\delta$	216×256×161	8.72	3.68	0.153~4.57
V	400	17.7	7,070	11.0	$2\pi\delta \times \pi\delta$	288×360×201	8.72	3.27	0.150~4.97

The boundary condition for gas concentration is the Dirichlet type, $C = C_0$ at the wall and $C = C_{\text{int}}$ at the free surface. The concentration difference between the free surface and the bottom, $\Delta C = C_{\text{int}} - C_0$, is constant and always positive throughout the computations to discuss gas transport mechanism into turbulent fluid across the free surface. The effect of gas concentration on fluid density is ignored in this study, therefore, fluid density ρ is constant throughout the present computations.

The governing equations for the present DNS are the conservation of mass, momentum and passive scalar. These governing equations used in this study are normalized by the wall shear velocity, u_τ, water height, δ, concentration difference, ΔC, like

$$u_i^+ = \frac{u_i}{u_\tau}, \overline{C} = \frac{C}{\Delta C}, \overline{x_i} = \frac{x_i}{\delta}, \bar{t} = \frac{t}{\delta / u_\tau}, p^+ = \frac{p/\rho}{u_\tau^2}. \tag{6}$$

After these normalizations are made, we obtain the nondimensional version of the governing equations,

$$\begin{aligned} &\frac{\partial u_\alpha}{\partial x_\alpha} = 0, \\ &\frac{\partial u_i}{\partial t} = \frac{\partial}{\partial x_\alpha}\left(\frac{1}{\mathrm{Re}}\frac{\partial u_i}{\partial x_\alpha} - u_\alpha u_i\right) - \frac{\partial p}{\partial x_i}, \\ &\frac{\partial C}{\partial t} = \frac{\partial}{\partial x_\alpha}\left(\frac{1}{\mathrm{Re}\cdot \mathrm{Sc}}\frac{\partial C}{\partial x_\alpha} - u_\alpha C\right). \end{aligned} \tag{7}$$

The Greek subscripts follow the summation convention in this report, while the Roman alphabets signify the component of vector quantities. We drop all the overbars and superscripts + for simplicity of description of these equations. The two nondimensional parameters, the Reynolds and the Schmidt numbers, appear in the normalized governing equations and determine nature of turbulence and turbulent gas transport.

We perform five simulations of free-surface turbulence by changing the friction Reynolds number from 150 to 400, corresponding to the bulk Reynolds number from about 2,290 to 7,070. These Reynolds numbers of the present DNS cover a large part of our previous laboratory experiments, $2{,}600 < \mathrm{Re}_m < 12{,}200$. The Schmidt number used in the present study is 1, rather than introducing the actual Schmidt number of CO_2, $\mathrm{Sc} \approx 580$, because of limitation of computer resources[6]. The employment of the virtual Schmidt number

for the present DNS has been justified by our previous studies[10]. We can compare gas fluxes obtained by both the laboratory and numerical experiments by using the calibrated Sherwood number $\mathrm{ShSc}^{-1/2}$, instead of using Sh. Table 1 summarizes the outline of the present five DNS.

The governing equations are approximated by a second-order finite difference method on a Cartesian staggered grid. An improved version of a fractional step method by Choi and Kim[11] is applied to link the velocities and the pressure without introducing a scalar potential. The equations are advanced in time by a four-stage fractional step procedure with a third-order Runge-Kutta integration scheme for nonlinear terms and a second-order Crank-Nicolson scheme for linear terms with an upper limit of the CFL number of $3/2 \sim \sqrt{3}$. All the elliptic type finite-difference equations for three velocity components, pressure and gas concentration are solved by a direct Poisson solver based on the fast Fourier transforms (FFT) and the Gaussian elimination.

RESULTS AND DISCUSSIONS

Fully developed turbulence statistics

Figure 3 shows the effect of the Reynolds number on distribution of mean velocity profiles in a semi-logarithmic chart. The wall-normal coordinate is scaled by the viscous wall units as $x_3^+ = x_3 u_\tau / \nu$. Typical low-Reynolds number effects, for example, very short log layer away from the wall, if it exists at all especially in Runs I and II, and decrease of log-layer velocity with increasing the Reynolds number, are found in this figure. It should be mentioned that the mean velocity profile for Run V ($\mathrm{Re} = 400$) agrees well with the DNS result by Moser et al.[12] of $\mathrm{Re} = 395$ in a two-dimensional channel. Also, the decrease of B with increasing the Reynolds number is very clear in the present study, as well as the Moser et al.[12] numerical results.

Root-mean-square (rms) velocity fluctuations, u_i^{rms}, are defined by

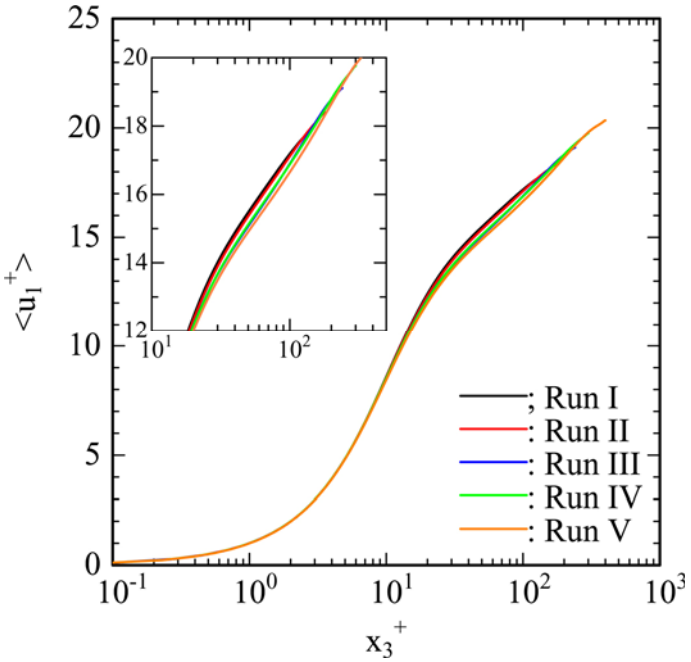

Figure 3: The effect of the Reynolds number on mean velocity profiles. The wall-normail coordinate is scaled as $x_3 u_\tau / \nu$.

$$u_i^{rms} = \langle u_i' u_i' \rangle^{1/2}, \tag{8}$$

where $u_i' = u_i - \langle u_i \rangle$ is the fluctuation from the ensemble average of velocity component u_i. The same rms profiles are plotted in Figure 4(a) and Figure **4**(b) for the all five cases by applying different scalings. The scaling used in Figure 4(a) is the viscous wall units, as introduced in Figure 3. In Figure 4(b), the wall-normal coordinate is scaled simply by x_3/δ. The peak values of the u_1^{rms} profiles in the all five cases are about $x_3^+ \approx 15$ in Figure 4(a), which are in excellent agreement with the laboratory measurements[3] and the previous numerical study in the near-wall turbulence by Moser et al.[12] The peak values are, however, influenced strongly by the Reynolds number, with their maxima changing from 2.61 at $\mathrm{Re} = 150$ to 2.70 at $\mathrm{Re} = 400$. This figure also exhibits that the effect of the Reynolds number enhances rms profiles in the whole of the flow domain for all the three velocity components. In Figure 4(b), rms velocity profiles are collapsed in the outer region of $x_3/\delta > 0.5$, hence, the effect of the Reynolds number on rms profiles is not distinctive there. The collapse of rms velocity profiles also suggests that characteristic thickness of the subsurface layer, which can be identified by increase of u_1^{rms} and u_2^{rms} profiles due to the intercomponent energy transfer[10], is independent with the Reynolds number if the wall-normal coordinate is scaled by δ. About 10% of the water

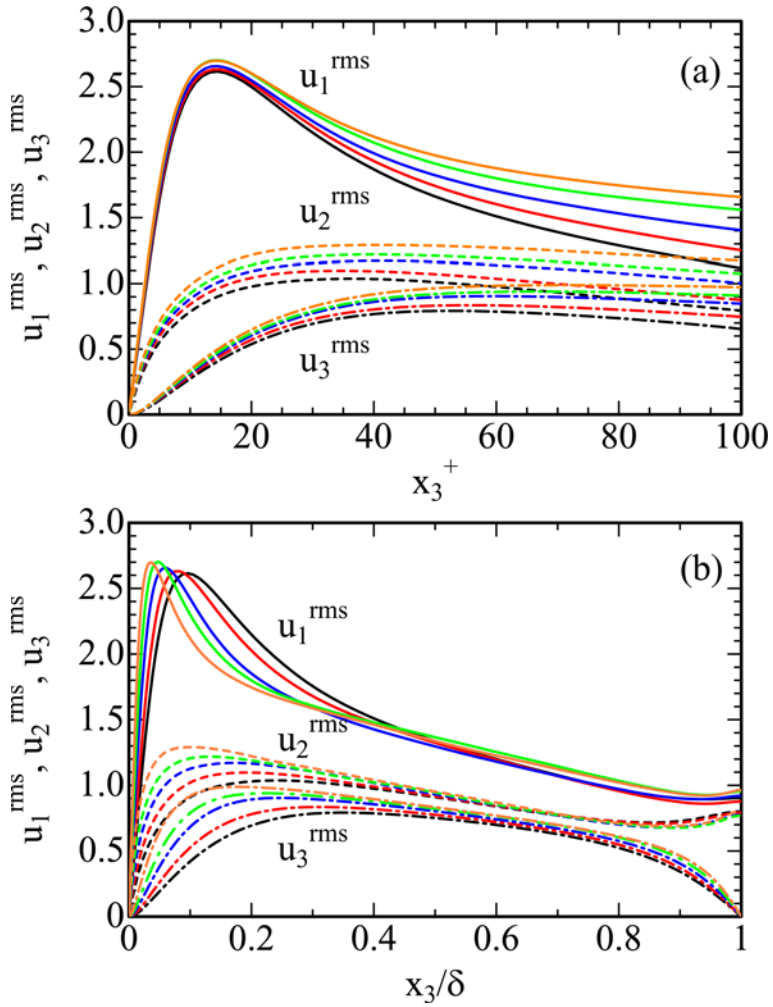

Figure 4: Root-mean-square velocity profiles obtained by the present DNS. The two different scalings on the wall-normal coordinate are applied; (a) scaled as $x_3 u_\tau/\nu$; (b) scaled as x_3/δ.

height adjacent to the free surface, $0.9 < x_3/\delta < 1.0$, is thought as characteristics thickness of the subsurface layer, therefore, the thickness scaled by wall shear velocity and fluid viscosity varies from about 15 at $\mathrm{Re} = 150$ to 40 at $\mathrm{Re} = 400$ in viscous wall units.

We decompose velocities and concentration as $u_i = \langle u_i \rangle + u_i'$ and $C = \langle C \rangle + C'$. Inserting these decompositions into the governing equations and take time-space average, the following the Reynolds average equations for momentum and gas transport are obtained

$$\begin{aligned} &\frac{\partial \langle u_i \rangle}{\partial t} + \langle u_j \rangle \frac{\partial \langle u_i \rangle}{\partial x_j} = \frac{\partial}{\partial x_j}\left(\frac{1}{\mathrm{Re}} \frac{\partial \langle u_i \rangle}{\partial x_j} - \langle u_j' u_i' \rangle \right), \\ &\frac{\partial \langle C \rangle}{\partial t} + \langle u_j \rangle \frac{\partial \langle C \rangle}{\partial x_j} = \frac{\partial}{\partial x_j}\left(\frac{1}{\mathrm{Re} \cdot \mathrm{Sc}} \frac{\partial \langle C \rangle}{\partial x_j} - \langle u_j' C' \rangle \right). \end{aligned} \tag{9}$$

Since the velocity and concentration fields are fully developed in the two wall-parallel directions, Eq. (9) is simplified as

$$\begin{aligned} &\frac{1}{\mathrm{Re}} \frac{\partial \langle u_1 \rangle}{\partial x_3} - \langle u_3' u_1' \rangle = 1 - \overline{x_3}, \\ &\frac{1}{\mathrm{Re} \cdot \mathrm{Sc}} \frac{\partial \langle C \rangle}{\partial x_3} - \langle u_3' C' \rangle = 1, \end{aligned} \tag{10}$$

where normalization by the friction concentration, $C_\tau = Q/u_\tau$, is used in Eq. (10). Both the distributions of the Reynolds stress and turbulent gas flux are plotted in Figure 5(a) and Figure **5**(b), as well as the profiles of the total momentum and gas fluxes. It is clear from the two figures that the results of the present DNS satisfy Eq. (10), verifying suitability of the fully developed velocity and concentration fields. Also, it is clear that the effect of the Reynolds number decreases thickness of both the near-wall and subsurface layers.

Gas transfer coefficient

Gas flux, Q, at the free surface in laboratory experiments is evaluated by gas flow rate, V, absorbed into turbulent water measured by a soap-film meter as

$$Q = \frac{V}{A}, \tag{11}$$

where A is the area of free surface in contact with CO_2. On the other hand, gas flux in numerical experiments can be estimated by the definition of flux based on the Fick's law of diffusion,

$$Q = D\left(\frac{\partial \langle C \rangle}{\partial x_3} \right)_{x_3 = \delta}, \tag{12}$$

where D is the molecular diffusivity of gas. The gas transfer coefficient is computed by substituting Eq. (12) into Eq. (5) as

$$K \equiv \frac{Q}{\Delta C} = \frac{D}{\Delta C}\left(\frac{\partial \langle C \rangle}{\partial x_3} \right)_{x_3 = \delta}. \tag{13}$$

The coefficient is normalized by the water depth, δ, and molecular diffusivity, D, as

$$\mathrm{Sh} = \frac{K\delta}{D}, \tag{14}$$

for convenience of comparison between the experimental and numerical results on gas fluxes. The normalized gas transfer coefficient is referred to as the Sherwood number. It is easy to confirm that Sh is the normalized gas concentration gradient at the free surface

$$\mathrm{Sh} = \left(\frac{\partial \langle \overline{C} \rangle}{\partial \overline{x}_3} \right)_{x_3=\delta} . \tag{15}$$

In this section, the attention is focused on comparison of the gas transfer coefficients obtained by the laboratory and present numerical experiments. Our previous laboratory experiments on gas transfer at the free surface are indicated in Figure 6 as a function of the bulk Reynolds number, Re_m, by closed circles. The Sherwood number in the turbulent open channel can be correlated by the following equation

$$\mathrm{ShSc}^{-1/2} = 1.70 \times 10^{-3} \mathrm{Re}_m^{\,1.007} . \tag{16}$$

This figure suggests that the normalized gas transfer coefficient is proportional to the Reynolds

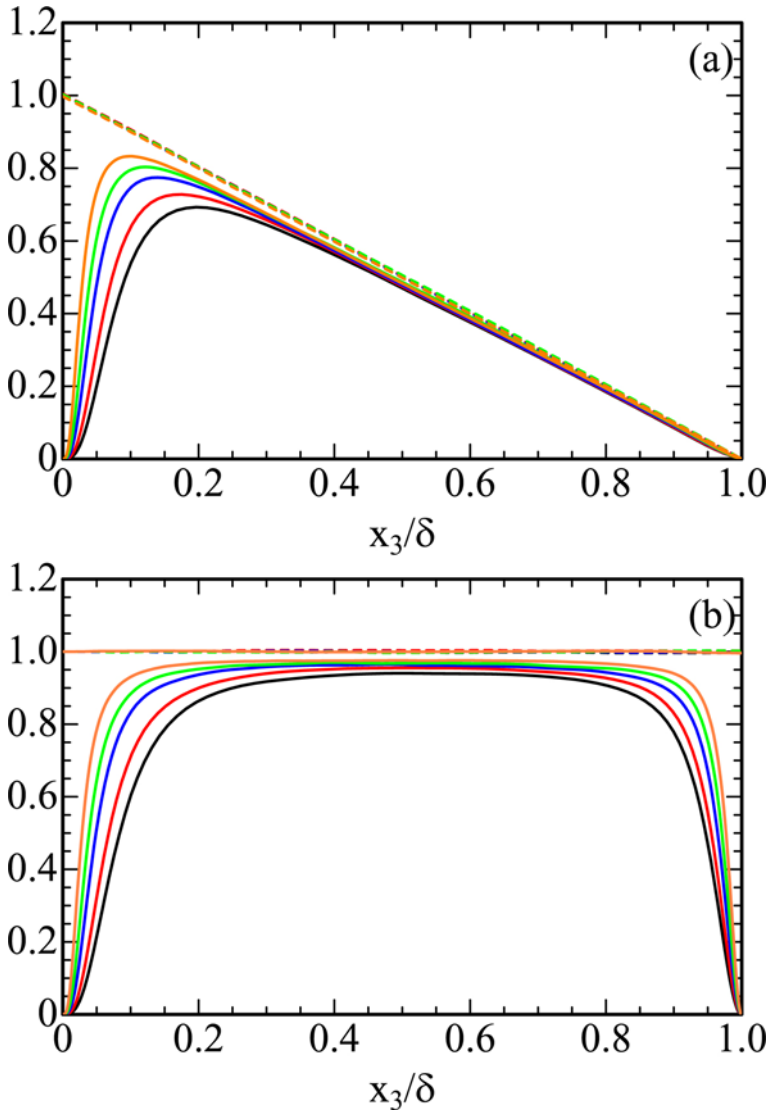

Figure 5: Wall-normal distributions of (a) the Reynolds stress; (b) the turbulent gas flux. The turbulent fluxes are plotted by solid lines while total fluxes are signified by dashed lines.

number, $\mathrm{ShSc}^{-1/2} \propto \mathrm{Re}_m$, is satisfied in the case of gas transfer at the free surface in turbulent open channel. The results of the present DNS are also plotted in the same figure by open circles. The numerically predicted Sherwood numbers agree well with the results of the previous laboratory measurements, nevertheless, their dependence on the Reynolds number is different. The present DNS predicts that the Sherwood number is expressed by

$$\mathrm{ShSc}^{-1/2} = 1.42\times10^{-2}\,\mathrm{Re}_m^{\,0.746}, \tag{17}$$

therefore, $\mathrm{ShSc}^{-1/2} \propto \mathrm{Re}_m^{\,3/4}$ is claimed by the present numerical simulations.

Rashidi et al.[2] measured the fraction of free-surface area covered by the surface patches, A_P/A, and the mean patch residence time at the free surface, T_P, to establish their correlation between the gas transfer coefficient and the subsurface hydrodynamics. They introduced the concept of the surface renewal to link the mean patch residence time and the gas transfer coefficient like,

$$K = \left(\frac{A_P}{A}\right)\left(\frac{D}{T_P}\right)^{1/2}, \tag{18}$$

and obtained

$$\frac{K\mathrm{Sc}^{1/2}}{(u_\tau U_m)^{1/2}} = 7.7\times10^{-3}. \tag{19}$$

Normalizing Eq. (19) as $\mathrm{Sh} = K\delta/D$, $\mathrm{Re}_m = U_m\delta/\nu$ and $\mathrm{Re} = u_\tau\delta/\nu$,

$$\frac{\mathrm{ShSc}^{-1/2}}{(\mathrm{Re}_m\,\mathrm{Re})^{1/2}} = 7.7\times10^{-3}, \tag{20}$$

is derived. The employment of the Dean's relation[7] for the viscous wall friction, Eqs. (1)-(3), is used to rewrite Eq. (20) as

$$\mathrm{ShSc}^{-1/2} = 3.22\times10^{-3}\,\mathrm{Re}_m^{\,15/16}. \tag{21}$$

The relation of Eq. (21) is also plotted by a chain-dotted line in Figure 6. It should be mentioned that the two independent laboratory experiments by Komori et al.[3] and Rashidi et al.[2] agree well with each other. The exponents of Re_m in the two correlations of Eqs. (16) and

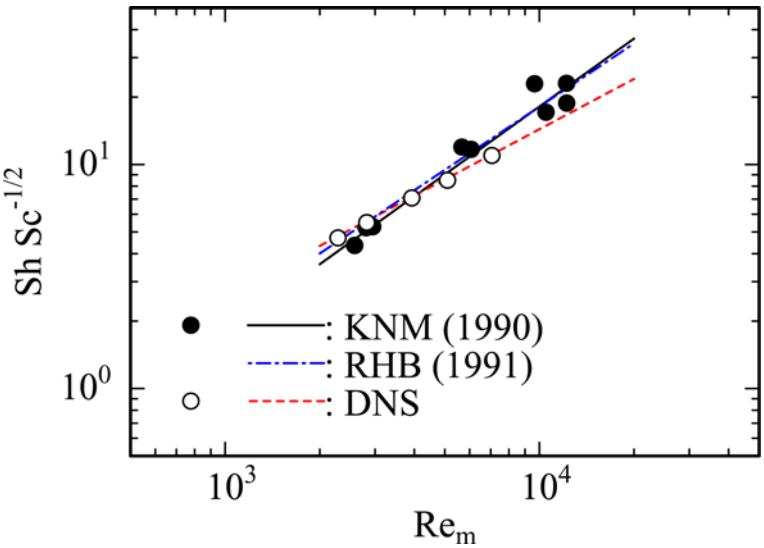

Figure 6: The relation between the Sherwood number, Sh, and the bulk Reynolds number, Re_m.

(21) are very close ($15/16 \approx 0.947$), hence, Rashidi et al.'s experiments confirm adequacy of our previous measurements on the gas transfer coefficients.

Figure 7 compares the results of laboratory measurements with those by the present DNS based on the Rashidi et al.'s correlation[2], Eq. (20). While the results of the laboratory experiments by Komori et al.[4] seem to satisfy Eq. (20), the predicted Sh by the present DNS deviates from Eq. (20) slightly, underestimating the gas transfer coefficient. Several reasons could be pointed out to explain this discrepancy. One is an error which seems to be inevitable in the laboratory experiments during the measuring process of gas fluxes at the free surface. A very slight contact of the plastic box to the free surface through very thin water film may produce small-scale perturbation on the water surface, resulting possibly an overestimation of gas fluxes. The other reason may be the effect of the side walls on turbulence under the free surface. The interaction of the side walls with water flow in experimental flume establish turbulence eddies in addition to those produced by the interactions of main flow with the bottom. The effect of the side walls could also be a reason of overestimating gas fluxes. While a numerical error which damps small-scale turbulence by truncation in finite-difference approximation could underestimate the concentration gradient at the free surface, the truncation error is not considered critical in the present numerical predictions. Handler et al. predicted the Sherwood number in a turbulent open channel flow of $\mathrm{Re} = 180$ based on a pseudospectral simulation, which represents very accurate nature of small-scale turbulence with very small truncation effect. The Handler et al. result[13], $\mathrm{ShSc}^{-1/2} \approx 5.4$, is very close to the present predictions of $\mathrm{ShSc}^{-1/2} = 5.50$, therefore, the present predictions of the Sherwood number is considered reliable. It is very difficult to give convincible explanation on the discrepancy between the results of the laboratory experiments and those by the numerical predictions so far, because these differences are small. In addition, the experimental results scatter among individual experimental runs. It should be stressed here that the discrepancy of the Sherwood numbers between the laboratory experiments and the numerical prediction are small, and acceptable practically as a margin of errors.

NEW PROPOSAL FOR CHARACTERISTIC TIME SCALE

We introduce the surface divergence to quantify the free-surface activity and to predict

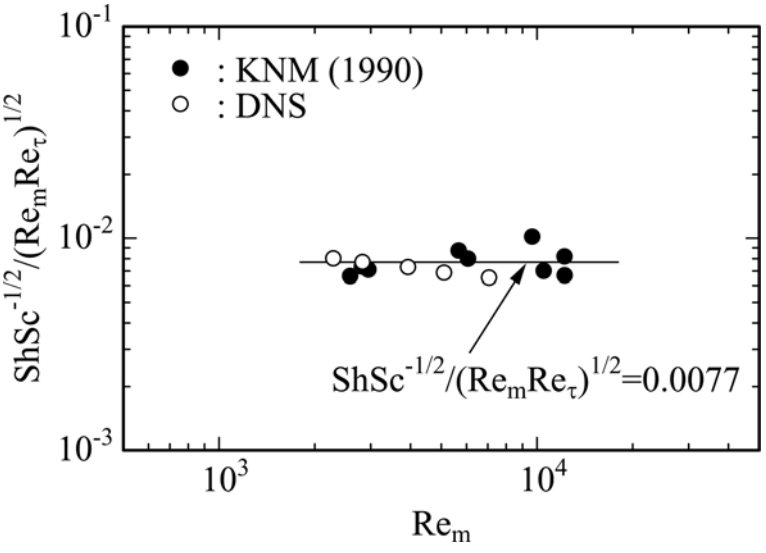

Figure 7: Comparison of the Sherwood numbers obtained by the laboratory experiments[3,4] with those by the present DNS based on the correlation by Rashidi et al.[2]

exactly the gas flux following the idea of the surface renewal. The surface divergence, S, is defined by the following equation

$$S \equiv \left(\frac{\partial u_1}{\partial x_1} + \frac{\partial u_2}{\partial x_2} \right)_{x_3=\delta} = -\left(\frac{\partial u_3}{\partial x_3} \right)_{x_3=\delta}, \tag{22}$$

because of the continuity of fluid, $\partial u_\alpha / \partial x_\alpha = 0$ (again, the Greek subscript follows the summation convention). It is recognized very widely that the surface divergence is one of the appropriate measures to quantify the free surface activity, since S is associated with the splat and anti-splat events[8]. It is reasonable to speculate that the surface divergence is linked physically to the instantaneous gas flux at the free surface. Indeed, the joint probability density distributions of the instantaneous gas concentration gradient and the surface divergence, as illustrated in Figure 8, verifies that the two parameters have a positive correlation. The correlation coefficients between the two parameters are about 0.75 in the all five DNS cases, and the statistical relation of the two parameters is considered large. In fact, a comparison of instantaneous distributions of the surface divergence and the gas concentration gradient at the free surface shown in Figure 9 support adequacy of the surface divergence to quantify the gas fluxes at the free surface.

The characteristic time scale for the surface divergence is evaluated based on its two-point correlation in the streamwise direction by the following procedure. First, the two-point correlation is computed by

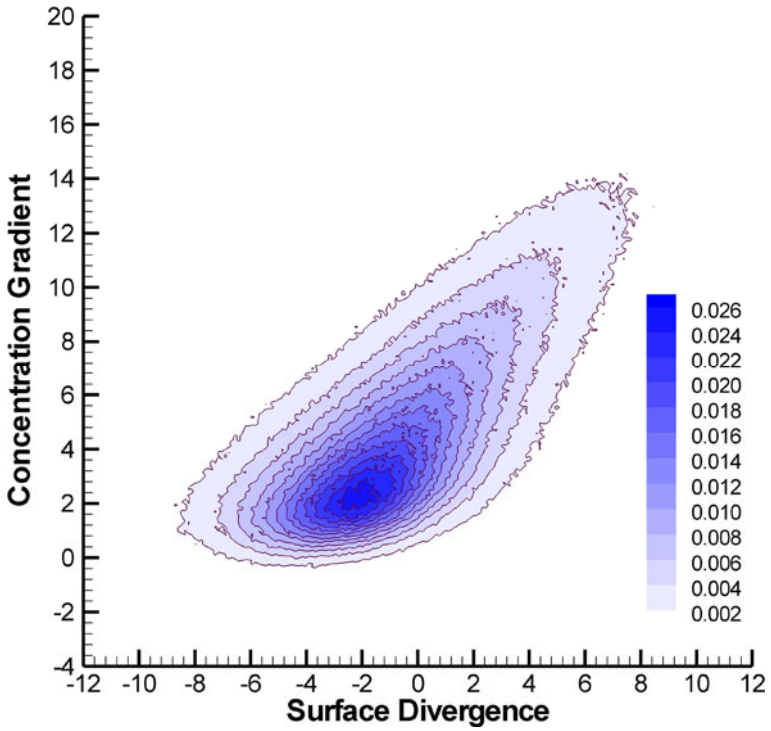

Figure 8: The joint probability density distribution of the surface divergence and the instantaneous gas concentration gradient at the free surface at $\mathrm{Re} = 180$ (Run II).

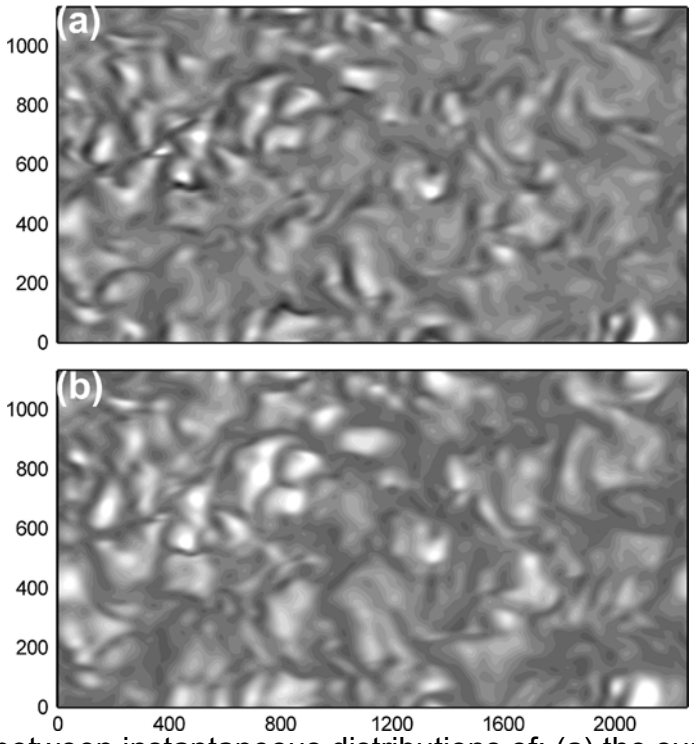

Figure 9: Comparison between instantaneous distributions of: (a) the surface divergence and: (b) the gas concentration gradient at a free surface for $\mathrm{Re} = 180$ (Run II). White in each figure indicates larger values.

$$R_1(\Delta x_1) = \frac{\langle S(x_1, x_2) S(x_1 + \Delta x_1, x_2) \rangle}{S^{rms} S^{rms}}, \tag{23}$$

to estimate the characteristic length scale of the surface divergence, where S^{rms} is root-mean-square of S. The distance Δx_1 where $R_1(\Delta x_3)$ is zero-correlated (i.e., $R_1(\Delta x_3) = 0$) is regarded as half of the length scale, L_S. A typical example of the two-point correlation distribution for $\mathrm{Re} = 180$ is indicated in Figure 10, and zero-correlated length is shown in the same figure by the dotted vertical line. Next, the characteristic time scale of the surface divergence is estimated using the mean velocity at the free surface, U_{surf}, as

$$T_S = \frac{L_S}{U_{surf}}. \tag{24}$$

The surface renewal assumption by Dankwerts[1] shows that the gas transfer coefficient is correlated by the characteristic time scale, T_S,

$$K \propto \left(\frac{D}{T_S} \right)^{1/2}. \tag{25}$$

The following relation is obtained by the nondimensionalization of Eq. (25)

$$\mathrm{ShSc}^{-1/2} \propto \left(\frac{\mathrm{Re}}{\overline{T_S}} \right)^{1/2}, \tag{26}$$

where $\overline{T_S} = T_S u_\tau / \delta$ is the normalized characteristic time scale for the surface divergence.

Figure 11 depicts the relation between the characteristic time scale and the Sherwood number obtained by the present numerical prediction (the results at $\mathrm{Re} = 400$ is yet to be processed for this analysis, and the results of Runs I-IV are only plotted). As expected, the results of the present numerical prediction suggest that the Sherwood number can be predicted by

$$\mathrm{ShSc}^{-1/2} = a\left(\frac{\mathrm{Re}}{\overline{T_S}}\right)^{1/2}, \tag{27}$$

where a is the constant and $a \approx 1/9$ is obtained. Eq. (27) satisfies the concept of the surface renewal, as indicated by Eq. (26), therefore, Figure 11 justifies suitability of the surface divergence to correlate the gas flux at the free surface following the concept of the surface renewal. The newly proposed procedure to determine the characteristic time scale for evaluation of the gas flux is advantageous compared with the previous VITA technique, since no arbitral parameter to be optimized is involved there.

CONCLUDING REMARKS

The mechanism of gas transfer into a turbulent liquid across a shear-free gas liquid interface (or free surface) has been investigated by means of a direct numerical simulation of turbulent open channel flows. The gas transfer coefficients were evaluated by the ensemble-averaged concentration gradient at the free surface and compared them with those by the laboratory experiments. The results of this comparison exhibited that the numerically predicted Sherwood numbers, which are the nondimensional form of the gas transfer coefficient, agree well with the experimental results. The experimental results exhibited that $\mathrm{ShSc}^{-1/2} \propto \mathrm{Re}_m$ is satisfied in the gas absorption experiments, while $\mathrm{ShSc}^{-1/2} \propto \mathrm{Re}_m{}^{3/4}$ is found by the present numerical predictions. The difference of the exponents in both the numerical and laboratory experiments is attributable to overestimation of the Sherwood number in the laboratory experiments, particularly at the large Reynolds number regime. Several reasons for this

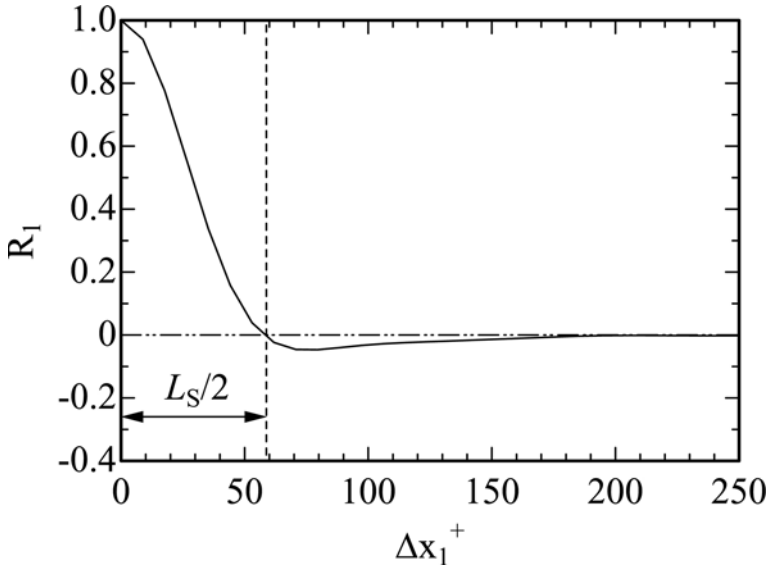

Figure 10: A typical example of the two-point correlation distribution of the surface divergence in the streamwise direction at $\mathrm{Re} = 180$ (Run II). The decorrelation length is shown by the vertical dotted line.

discrepancy between the laboratory and numerical experiments are considered. One is an effect of small-scale perturbation on the free surface in the laboratory experiments produced by the plastic box contacting very slightly to the free surface. The gas transfer coefficient at the free surface may increase unphysically by the effect of such small-scale perturbation. A numerical error produced by truncation for evaluations of spatial derivatives is, on the other hand, not considered critical in the present simulation, since the predicted Sherwood number in this study is confirmed very close to that computed by the other separated numerical study, whose numerical technique involves negligible truncation effect.

The determination of the characteristic time scale based on the two-point correlation of the surface divergence was discussed using the turbulent flow realization obtained by the present DNS. The relation between the time scale and the Sherwood number reveals that the surface divergence is suitable to define the characteristic time scale for exact prediction of the gas flux at the free surface, following the assumption of the surface renewal. The proposed determination of the characteristic time scale could be an alternative to the previous VITA method, since no arbitral parameter is employed in the proposed process.

The present discussion on the characteristic time scale at the free surface ignored many important physical phenomena such as surface contamination, density stratification and surface waves. An applicability of this method to various kinds of turbulent flows should be verified in the near future.

ACKNOWLEDGEMENTS

This study has been supported by the Research Council of Norway through the BeMatA project. The author would like thank to Dr. Guttorm Alendal at the Bergen Center of Computational Science (BCCS), the University of Bergen, Norway, for his support to this study, especially development of the DNS code. The author has also been supported financially by the Institute of Environmental Management Technology (EMTech), the National Institute of Advanced Industrial Science and Technology (AIST).

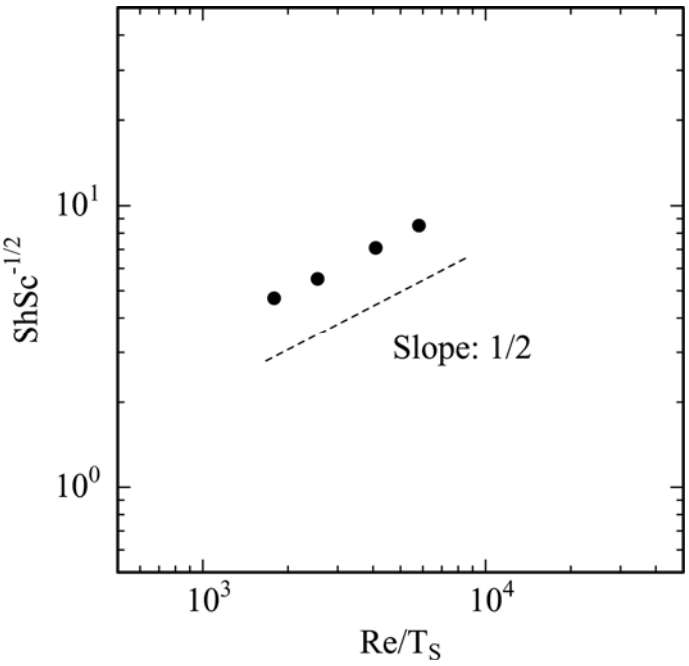

Figure 11: Suitability of the characteristic time scale of the surface divergence for estimation of the gas flux at the free surface based on the idea of the surface renewal approximation.

LITERATURE CITED.

1. Dankwerts, P. V., "Significance of liquid-film coefficients in gas absorption," *Ind. Engng. Chem* **43**, 1460-1467 (1951).
2. Rashidi, M., Hetsroni, G. and Banerjee, S., "Mechanisms of heat and mass transport at gas-liquid interfaces, " *Int. J. Heat Mass Transf.* **34**, 1799-1810 (1991).
3. Komori, S., Murakami, Y. and Ueda, H., "The relationship between surface-renewal and bursting motions in an open-channel," *J. Fluid Mech.* **203**, 103-123 (1989).
4. Komori, S., Nagaosa, R. and Murakami, Y., "Mass transfer into a turbulent liquid across the zero-shear gas-liquid interface," *AIChE J.* **36**, 957-960 (1990).
5. Rashidi, M., "Burst-interface interactions in free surface turbulent flows," *Phys. Fluids* **9**, 3485-3501 (1997).
6. Nagaosa, R. and Handler, R. A., "Statistical analysis of coherent vortices near a free surface in a fully developed turbulence," *Phys. Fluids* **15**, 375-394 (2003).
7. Blackwelder, R. F. and Kaplan, R. E, "On the wall structure of the turbulent boundary layer," *J. Fluid Mech.* **76**, 89-112 (1976).
8. Handler, R. A., Leighton, R. I., Smith, G. B. and Nagaosa, R., "Surfactant effects on passive scalar transport in a fully developed turbulent flow," *Int. J. Heat Mass Transf.* **46**, 2219-2238 (2003).
9. Dean, R. B., "Reynolds number dependence of skin friction and other bulk flow variables in two-dimensional rectangular duct flow," *ASME J. Fluid Engng.*, **100**, 215-223 (1978).
10. Nagaosa, R., "Direct numerical simulation of vortex structures and turbulent scalar transfer across a free surface in a fully developed turbulence," *Phys. Fluids* **11**, 1581-1595 (1999).
11. Choi, H. and Moin, P., "Effects of computational time step on numerical solutions of turbulent flow," *J. Comput. Phys.* **113**, 1-4 (1994).
12. Moser, R., Moin, P. and Kim, J., "Direct numerical simulation of turbulent flow up to $\mathrm{Re}_\tau = 590$," *Phys. Fluids* **11**, 943-946 (1999).
13. Handler, R. A., Saylor, J. R., Leighton, R. I. and Rovelstad, A. L., "Transport of a passive scalar at a shear-free boundary in fully developed turbulent open channel flow," *Phys. Fluids* **11**, 2607-2625 (1999).